

# A precision measurement of electroweak parameters in neutrino-nucleon scattering

CCFR/NuTeV Collaboration

K. S. McFarland<sup>3</sup>, C. G. Arroyo<sup>2</sup>, B. J. King<sup>2</sup>, L. de Barbaro<sup>5</sup>, P. de Barbaro<sup>7</sup>, A. O. Bazarko<sup>2</sup>, R. H. Bernstein<sup>3</sup>, A. Bodek<sup>7</sup>, T. Bolton<sup>4</sup>, H. Budd<sup>7</sup>, L. Bugel<sup>3</sup>, J. Conrad<sup>2</sup>, R. B. Drucker<sup>6</sup>, D. A. Harris<sup>7</sup>, R. A. Johnson<sup>1</sup>, J. H. Kim<sup>2</sup>, T. Kinnel<sup>8</sup>, M. J. Lamm<sup>3</sup>, W. C. Lefmann<sup>2</sup>, W. Marsh<sup>3</sup>, C. McNulty<sup>2</sup>, S. R. Mishra<sup>2</sup>, D. Naples<sup>4</sup>, P. Z. Quintas<sup>2</sup>, A. Romosan<sup>2</sup>, W. K. Sakumoto<sup>7</sup>, H. Schellman<sup>5</sup>, F. J. Sciulli<sup>2</sup>, W. G. Seligman<sup>2</sup>, M. H. Shaevitz<sup>2</sup>, W. H. Smith<sup>8</sup>, P. Spentzouris<sup>2</sup>, E. G. Stern<sup>2</sup>, M. Vakili<sup>1</sup>, U. K. Yang<sup>7</sup>, and J. Yu<sup>3</sup>, G. P. Zeller<sup>5</sup>

<sup>1</sup> University of Cincinnati, Cincinnati, OH 45221, USA<sup>2</sup> Columbia University, New York, NY 10027, USA<sup>3</sup> Fermi National Accelerator Laboratory, Batavia, IL 60510, USA<sup>4</sup> Kansas State University, Manhattan, KS 66506, USA<sup>5</sup> Northwestern University, Evanston, IL 60208, USA<sup>6</sup> University of Oregon, Eugene, OR 97403, USA<sup>7</sup> University of Rochester, Rochester, NY 14627, USA<sup>8</sup> University of Wisconsin, Madison, WI 53706, USA

Received: 5 August 1997

**Abstract.** The CCFR collaboration reports a precise measurement of electroweak parameters derived from the ratio of neutral-current to charged-current cross-sections in neutrino-nucleon scattering at the Fermilab Tevatron. We determine  $\sin^2 \theta_W^{\text{(on-shell)}} = 0.2236 \pm 0.0028(\text{expt.}) \pm 0.0030(\text{model})$  for  $M_{\text{top}} = 175$  GeV,  $M_{\text{Higgs}} = 150$  GeV. This is equivalent to  $M_W = 80.35 \pm 0.21$  GeV. The good agreement of this measurement with Standard Model expectations implies the exclusion of additional  $\nu\nu q q$  contact interactions at 95% confidence at a mass scale of 1-8 TeV, depending on the form of the contact interaction.

In the early 1980's, accurate measurements of neutrino neutral-current scattering cross-sections provided key input to the Standard Model's predictions of the  $W$  and  $Z$  boson masses. Even with the production of copious on-shell  $W$  and  $Z$  bosons at high luminosity  $p\bar{p}$  and  $e^+e^-$  colliders, neutrino-nucleon ( $\nu N$ ) scattering still provides a measurement of electroweak parameters, in particular  $M_W/M_Z$ , with comparable precision. More importantly, the high precision comparison among these distinct electroweak processes differing in  $q^2$  by more than two orders of magnitude provides a critical test of the theory and the possibility to search for non-Standard Model contributions with very high mass scales or low probabilities [1–3]. The measurement presented here represents the most precise determination of  $\sin^2 \theta_W$  from  $\nu N$  scattering to date and supersedes the previous result from CCFR [4] due to increased statistics and improved evaluation of systematic errors.

The neutral-current (NC) and charged-current (CC)  $\nu N$  deep inelastic scattering differential cross-sections on an isoscalar target of light quarks are related by

$$\frac{d}{dx dq^2} \left( \sigma_{\text{NC}}^{\nu, \bar{\nu}} \right) = (u_L^2 + d_L^2) \frac{d}{dx dq^2} \left( \sigma_{\text{CC}}^{\nu, \bar{\nu}} \right)$$

$$+ (u_R^2 + d_R^2) \frac{d}{dx dq^2} \left( \sigma_{\text{CC}}^{\bar{\nu}, \nu} \right) \quad (1)$$

where  $u_{L,R}$  and  $d_{L,R}$  are the left(L) and right(R)-handed couplings of the  $Z^0$  to up and down quarks, respectively. Small corrections to (1) arise from massive quark production suppression, CKM matrix effects, higher-twist processes, electromagnetic and electroweak radiative corrections, and from any isovector component in the target, including heavy quark seas. Within the Standard Model, these left and right-handed couplings are given by  $I_{\text{Weak}}^{(3)} - Q_{\text{EM}} \sin^2 \theta_W$  and  $-Q_{\text{EM}} \sin^2 \theta_W$ , respectively, allowing a measurement of  $\sin^2 \theta_W$  from ratios of NC to CC, and  $\nu$  to  $\bar{\nu}$  CC cross-sections. Furthermore, if the expression for  $\sigma_{\text{NC}}^{\nu}$  in (1) is used to extract  $\sin^2 \theta_W$ , it is almost equal to  $\sin^2 \theta_W$  in the “on-shell” renormalization scheme ( $\sin^2 \theta_W^{\text{(on-shell)}} \equiv 1 - M_W^2/M_Z^2$  to all orders), independent of  $M_{\text{top}}$  and  $M_{\text{Higgs}}$  [5, 6]. Therefore, the measurement of  $\sin^2 \theta_W$  from  $\nu N$  scattering, combined with the precise measurements of  $M_Z$  from LEP [7], implies a measurement of  $M_W$ . In addition, direct extraction of  $u_{L,R}$  and  $d_{L,R}$  also allows a search for a variety of non-Standard

Model processes through comparison of the measurements from  $\nu N$  scattering with Standard Model expectations.

The CCFR detector consists of an 18 m long, 690 ton neutrino target calorimeter with a mean density of  $4.2 \text{ g/cm}^3$ , followed by an iron toroid spectrometer. The target calorimeter consists of 168 iron plates,  $3\text{m} \times 3\text{m} \times 5.1\text{cm}$  apiece. The active elements are liquid scintillation counters spaced every two plates (10.2 cm of steel) and drift chambers spaced every four plates (20.4 cm of steel). There are a total of 84 scintillation counters and 42 drift chambers in the target. The neutrino target is approximately isoscalar, with a 5.67% neutron excess. The toroid spectrometer is not directly used in this analysis.

The Fermilab Tevatron Quadrupole Triplet neutrino beam is created by decays of pions and kaons produced when 800 GeV protons hit a BeO target. A wide band of secondary energies is accepted by downstream focusing magnets. The target is located about 1.4 km upstream of the neutrino detector. The target and focusing train are followed by a 0.5 km decay region. The interactions of the beam are predominantly from muon neutrinos (86%) and anti-neutrinos (12%), but also include a small fraction of electron neutrinos (2.3%). The mean energies of the  $\nu_\mu$ ,  $\bar{\nu}_\mu$ , and  $\nu_e(\bar{\nu}_e)$  events are 165, 135 and 160 GeV, respectively. The mean  $q^2$  exchanged in the neutrino interactions used in this analysis was  $-35 \text{ GeV}^2$ .

Neutrinos are observed *via* their NC and CC interactions, both of which are selected in this analysis from the energy transferred to the struck quark which appears as a hadronic shower in the target calorimeter. The hadronic energy is measured by the variable  $E_{\text{cal}}$ , which is the sum of energies observed in the first 20 scintillation counters (2.1m equivalent of steel) in the target downstream of the interaction vertex. NC events usually have no final-state muon and deposit energy over a range of counters typical of a hadronic shower (5 to 20 counters).  $\nu_\mu$  CC events are distinguished by the presence of a muon in the final state which deposits energy typical of a minimum ionizing particle in a large number of consecutive scintillation counters downstream of the hadronic shower.

A “length” is defined for each event as the number of counters between the interaction vertex and the last counter consistent with the energy deposition expected from a single muon passing through the calorimeter. Events with a “short” length are identified as NC candidates. The separation between short and “long” events is made at 20 counters (2.1m of steel) for events with  $E_{\text{cal}} \leq 45 \text{ GeV}$ , 25 counters (2.6m of steel) for events with  $45 < E_{\text{cal}} \leq 100 \text{ GeV}$ , and 30 counters (3.1m of steel) for events with  $E_{\text{cal}} > 100 \text{ GeV}$ . As is shown in the length distributions in Fig. 1, NC interactions lie in a clear peak, well-below the length cut, with a continuous band of CC  $\nu_\mu$  interactions under the peak. The CC  $\nu_\mu$  background is calculated to be 10.5%, 21.3%, and 21.2% of the “short” NC candidates in the three  $E_{\text{cal}}$  regions, respectively.

The data used in this analysis were taken between 1984 and 1988 in FNAL experiments E-744 and E-770. Events were required to have  $E_{\text{cal}} > 20 \text{ GeV}$  to ensure full efficiency of the trigger [4]. Fiducial cuts were made on the

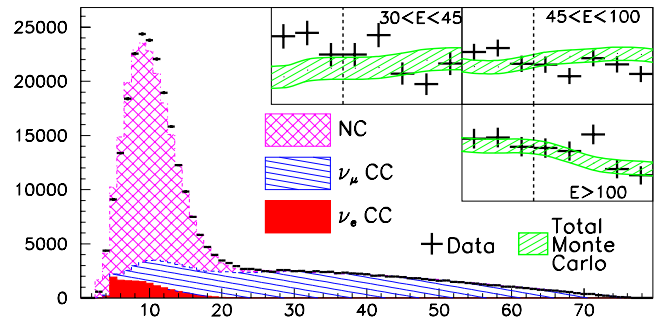


**Fig. 1.** Event length in data and Monte Carlo. The prediction for NC, CC  $\nu_\mu(\bar{\nu}_\mu)$ , and CC  $\nu_e(\bar{\nu}_e)$  interactions is shown. Inset are comparisons in the region of the length cut of data and Monte Carlo with systematic errors shown

location of the neutrino interaction in the calorimeter to ensure that events were neutrino-induced, that a separation between long and short events could be made, and that events originated in the central part of the calorimeter to maximize containment of wide-angle muons and to minimize the ratio of electron to muon neutrinos. The resulting data sample consisted of  $8.1 \times 10^5$  events, and from these events the ratio

$$R_{\text{meas}} = \frac{\# \text{ of short events}}{\# \text{ of long events}} = 0.4151 \pm 0.0010$$

was calculated.

A detailed Monte Carlo was used to determine electroweak parameters from  $R_{\text{meas}}$ . The only undetermined inputs to this Monte Carlo were the neutral current quark couplings which were then varied until the Monte Carlo predicted an  $R_{\text{meas}}$  which agreed with that observed in the data. For the extraction of  $\sin^2 \theta_W$ , the couplings in the Monte Carlo were fixed to their Standard Model predictions as functions of  $\sin^2 \theta_W$ , which was then varied as the only free parameter. The Monte Carlo included detector response and beam simulations, as well as a detailed cross-section model which included electroweak radiative corrections, isovector target corrections, heavy quark production and seas, the longitudinal cross-section, and lepton mass effects.

There are three major uncertainties in the comparison of  $R_{\text{meas}}$  from the Monte Carlo to the data: the statistical error in the data, the uncertainty in the effective charm quark mass for charged current charm production, and the uncertainty in the incident flux of  $\nu_e$ 's on the detector.

The charm quark mass error comes from the uncertainty in modeling the mass threshold of the charm production cross section. The Monte Carlo uses a slow-rescaling model with the parameters extracted using events with two oppositely charged muons (e.g.,  $\nu q \rightarrow \mu^- c$ ,  $c \rightarrow \mu^+ X$ ) from this experiment [8]. The shape and magnitude of the strange sea were also extracted in the same analysis and were used in the Monte Carlo cross-section model. This error dominates the calculation of  $R_{\text{meas}}$  at low  $E_\nu$  (and low  $E_{\text{cal}}$ ) where the threshold suppression is greatest.

The  $\nu_e(\bar{\nu}_e)$  flux uncertainty has an important effect on  $R_{\text{meas}}$  because almost all charged current  $\nu_e(\bar{\nu}_e)$  events

are short events. Therefore, the relatively small fractional uncertainty in the  $\nu_e(\bar{\nu}_e)$  flux is a significant effect, particularly at high  $E_{\text{cal}}$  since most  $\nu_e(\bar{\nu}_e)$  charged current interactions deposit the full incident neutrino energy into the calorimeter. Two techniques were used to determine the  $\nu_e(\bar{\nu}_e)$  flux. In both E744 and E770, a detailed beam Monte Carlo was used to predict the flux, up to a 4.1% uncertainty in each experiment. This 4.1% is dominated by a 20% production uncertainty in the  $K_L$  content of the secondary beam which produces 16% of the  $\nu_e$  flux. The bulk of the  $\nu_e$  flux comes from  $K_{e3}^{\pm}$  decays, which are well-constrained by the observed  $\nu_{\mu}$  spectrum from  $K_{\mu 2}^{\pm}$  decays [4]. In E770, the  $\nu_e(\bar{\nu}_e)$  flux was measured directly using the fact that CC  $\nu_e(\bar{\nu}_e)$  interactions will have a high fraction of their energy deposited in the first three counters downstream of the event vertex. This gave an independent measurement of the  $\nu_e(\bar{\nu}_e)$  flux with a uncertainty of 3.5% which was in good agreement with the Monte Carlo method [9]. Combining these techniques, a measurement of the  $\nu_e(\bar{\nu}_e)$  flux sum in E744 and E770 is obtained with a 2.9% error.

Other sources of experimental uncertainties were kept small through extensive modeling based on neutrino and testbeam data [10–12]. The cross-section model used a modified Buras-Gaemers parameterization [13] of the CCFR data for input parton distributions. This resulted in partial cancellations of certain systematic effects, such as errors in energy calibration. Systematic uncertainties associated with the measurement of  $E_{\text{cal}}$  include possible small NC/CC shower differences (constrained by a LEPTO Monte Carlo study [4]), uncertainties in the muon energy deposit within the hadron shower, uncertainties in the resolution function,  $e/\pi$  response, and absolute energy scales obtained from hadron and electron test beam measurements [10,11]. The length uncertainties include those associated with the shower length parameterizations of test beam measurements [12], the calorimeter longitudinal vertex determination (studied using the vertex from events with two muon tracks), counter inefficiencies and noise, and counter spatial dimensions. In the cross-section model, the level of the charm sea was taken from the CTEQ4L parton distribution functions and was assigned a 100% uncertainty. Our parameterization of  $R_{\text{long}} = \sigma_L/\sigma_T$  is based on QCD predictions and data from charged lepton scattering experiments [14] and is varied by 15% of itself to estimate uncertainties. A correction for the difference between  $u$  and  $d$  valence quark distributions in nucleons, obtained from muon scattering data [15], was applied to account for the 5.67% excess of neutrons over protons in the target.

A correction was also applied for the asymmetry in the  $u$  and  $d$  sea distributions suggested by the NA51 Drell-Yan data [16] and the Gottfried Sum Rule as measured in muon scattering [17]. Radiative corrections to the scattering cross-sections were applied using computer code supplied by Bardin [18] and 1-loop electroweak radiative corrections as calculated by Marciano and Sirlin [5]. Possible higher-twist corrections were parameterized in a VDM-based model of Pumplin [19] which was constrained by

**Table 1.** Uncertainties in the extraction of  $\sin^2 \theta_W^{\text{(on-shell)}}$  from the CCFR data

SOURCE OF UNCERTAINTY	$\delta \sin^2 \theta_W$
data statistics	0.0019
Monte Carlo statistics	0.0004
<b>TOTAL STATISTICS</b>	<b>0.0019</b>
$\nu_e$ flux	0.0015
Transverse Vertex	0.0004
Energy Measurement	
Hadron Energy Scale (1%)	0.0004
Muon Energy Loss in Shower	0.0003
Muon Energy Scale (1%)	0.0002
Event Length	
Hadron Shower Length	0.0007
Counter Efficiency and Noise	0.0006
Vertex Determination	0.0003
<b>TOTAL EXP. SYST.</b>	<b>0.0019</b>
Charm Production, $\bar{s}$ ( $M_c = 1.31 \pm 0.24$ GeV)	0.0027
Higher Twist	0.0010
Longitudinal Cross-Section	0.0008
Charm Sea, ( $\pm 100\%$ )	0.0006
Non-Isoscalar Target	0.0004
Structure Functions	0.0002
Rad. Corrections	0.0001
<b>TOTAL PHYSICS MODEL</b>	<b>0.0030</b>
<b>TOTAL UNCERTAINTY</b>	<b>0.0041</b>

lepto-production data. Table 1 shows the uncertainties in the determination of  $\sin^2 \theta_W$ .

The extraction of  $\sin^2 \theta_W^{\text{(on-shell)}}$  by comparing  $R_{\text{meas}}$  in the data to the Monte Carlo with  $\sin^2 \theta_W^{\text{(on-shell)}}$  as the single free parameter yields,

$$\begin{aligned} \sin^2 \theta_W^{\text{(on-shell)}} &= 0.2236 \pm 0.0028((\text{expt.}) \pm 0.0030(\text{model})) \\ &\quad + 0.0006 \times \left( \frac{(M_{\text{top}}^2 - (175 \text{ GeV})^2)}{(100 \text{ GeV})^2} \right) \\ &\quad - 0.0002 \times \log_e \left( \frac{M_{\text{Higgs}}}{150 \text{ GeV}} \right). \end{aligned} \quad (2)$$

The explicit dependence of the central value of this result on  $M_c$  is  $0.2236 + 0.0111 \times (M_c - 1.31 \text{ GeV})$ . Only data with  $E_{\text{cal}} > 30 \text{ GeV}$  was used in this result to reduce the effect of the charm-production and higher-twist systematics which are largest at low  $E_{\text{cal}}$ . Since  $\sin^2 \theta_W^{\text{(on-shell)}} \equiv 1 - M_W^2/M_Z^2$ , this result implies  $M_W = 80.35 \pm 0.21 \text{ GeV}$ . This value of  $M_W$  agrees with direct mass measurements [20] as shown in Fig. 2, and this result is also in good agreement both with previous  $\nu N$  measurements and with Standard Model expectations [7].

$R_{\text{meas}}$  is also used to extract a constraint on the couplings of quarks to the  $Z^0$ :

$$\begin{aligned} \kappa &= 0.5820 \pm 0.0041 = 1.7897g_L^2 + 1.1479g_R^2 \\ &\quad - 0.0916\delta_L^2 - 0.0782\delta_R^2, \end{aligned} \quad (3)$$

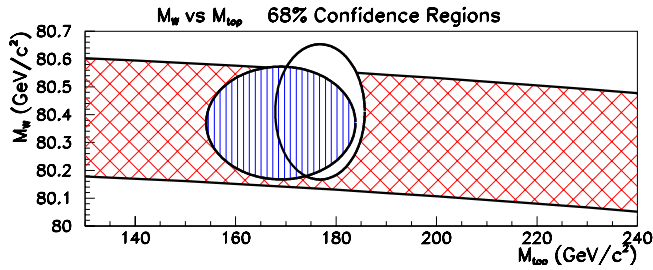


**Fig. 2.**  $M_W$  vs  $M_{\text{top}}$ . This measurement is shown as a cross-hatched band. CDF measurements provide the hollow ellipse, and the D0 measurements are shown in the striped ellipse

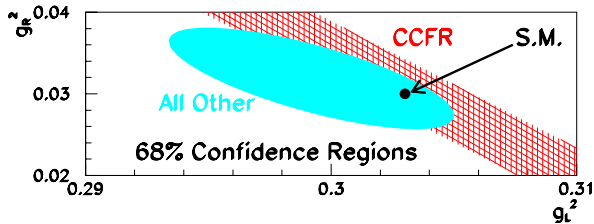


**Fig. 3.** One-sigma constraints on the isoscalar neutral current quark couplings,  $g_L^2$  and  $g_R^2$ , from this result (*hatched*) and from other neutrino data (*solid*)

where  $g_{L,R}^2 = u_{L,R}^2 + d_{L,R}^2$  and  $\delta_{L,R}^2 = u_{L,R}^2 - d_{L,R}^2$ . The explicit dependence of the central value of  $\kappa$  on  $M_c$  is  $\kappa = 0.5820 - (M_c - 1.31) \times 0.0111$ . The Standard Model prediction is  $\kappa = 0.5817 \pm 0.0013$  for the measured values of  $M_Z$ ,  $M_{\text{top}}$ ,  $M_W$ . Figure 3 compares this result to other neutrino data [21] and the Standard Model prediction [7].

Because the CCFR result for neutral-current quark couplings are in good agreement with Standard Model expectations, this result disfavors the introduction of additional processes contributing to the same final state. To quantify this, we use the CCFR data to constrain models of new  $\nu\nu qq$  contact interactions. Such models are often used to parameterize searches for fermion compositeness [22]. We assume a generation-universal interaction of the form

$$-\mathcal{L} = \sum_{H_q \in \{L,R\}} \frac{\pm 4\pi}{\left(\Lambda_{LH_q}^\pm\right)^2} \times \left\{ \bar{l}_L \gamma^\mu l_L \bar{q} H_q \gamma_\mu q H_q + l_L \gamma^\mu \bar{l}_L \bar{q} H_q \gamma_\mu q H_q + \bar{l}_L \gamma^\mu l_L q H_q \gamma_\mu \bar{q} H_q + l_L \gamma^\mu \bar{l}_L q H_q \gamma_\mu \bar{q} H_q \right\}. \quad (4)$$

Such interactions would shift one or more of the quark couplings in  $\nu$  or  $\bar{\nu}$  induced interactions from its Standard Model value [1]. Only limits for couplings to left-handed neutrinos (and right-handed couplings to anti-neutrinos) are given, since the charged-current weak interactions which produce the neutrinos in the beamline are assumed to have only Standard Model contributions. One-sided 95% confidence level lower limits for each  $\Lambda$  are set by finding the points in the space of measured couplings at which the  $\chi^2$  is 1.64 units above the minimum, and then determining the  $\Lambda$  to which these points

**Table 2.** 95% Confidence Lower Limits on mass scales of new  $\nu\nu qq$  contact terms from CCFR

Interaction	$\Lambda^+$	$\Lambda^-$
Neutrino Interactions Only		
LL	4.6 TeV	5.1 TeV
LR	4.1 TeV	4.3 TeV
LV	6.5 TeV	6.5 TeV
LA	2.1 TeV	3.2 TeV
Antineutrino Interactions Only		
LL	1.3 TeV	2.2 TeV
LR	3.8 TeV	4.0 TeV
LV	4.3 TeV	4.5 TeV
LA	3.1 TeV	3.7 TeV
Neutrino and Anti-Neutrino		
LL	5.0 TeV	5.4 TeV
LR	5.8 TeV	5.8 TeV
LV	7.9 TeV	7.8 TeV
LA	3.0 TeV	1.8 TeV

correspond in each model <sup>1</sup>. Limits for LL, LR, LV (vector,  $\Lambda_{LL} = \Lambda_{LR}$ ) and LA (axial-vector,  $\Lambda_{LL} = -\Lambda_{LR}$ ) are shown in Table 2. Limits are shown for the cases when this new contact term affects neutrinos interactions only, when it affects anti-neutrino interactions only, and when it affects both neutrino and anti-neutrino interactions. These limits are roughly comparable to the limits for charged lepton-quark interactions in  $p\bar{p}$  collider data from the Fermilab Tevatron [23].

In summary, CCFR has produced the most precise measurements of neutral-current neutrino-nucleon interactions to date, and has used these measurements to constrain neutral-current coupling to quarks. Within the Standard Model, this leads to a measurement of  $\sin^2 \theta_W^{\text{(on-shell)}} = 0.2236 \pm 0.0041$  ( $M_{\text{top}} = 175$  GeV,  $M_{\text{Higgs}} = 150$  GeV) which corresponds to  $M_W = 80.35 \pm 0.21$  GeV. This result is also used to limit possible TeV-scale contact interactions of neutrinos and quarks outside the Standard Model.

*Acknowledgements.* This research was supported by the U.S. Department of Energy and the National Science Foundation. We thank the staff of the Fermi National Accelerator Laboratory for their hard work in support of this experimental effort. We also wish to thank Bill Marciano for helpful suggestions regarding the presentation of the limits on new contact interactions.

<sup>1</sup> In the case of many of these computations, there are actually two solutions for such a  $\Lambda$ , one at comparatively high energy, and one at low energy where a cancellation among large changes in the individual quark chiral couplings results in no change in the measured quantity,  $\kappa$ , defined in (3). In each one of these cases, the changes in one or more of the individual couplings are so large that the possibility of such an interaction is already excluded by less precise data on individual quark chiral couplings [21]. Therefore, only the high-mass lower limits on  $\Lambda$  given by the procedure in the text are reported here

## References

1. P. Langacker et al., Rev. Mod. Phys. **64**, 87 (1991)
2. K. Hagiwara et al., Z. Phys. **C64**, 559 (1994)
3. K.S. McFarland, D. Naples et al., Phys. Rev. Lett., **75**, 3993 (1995)
4. C. Arroyo, B.J. King et al., Phys. Rev. Lett., **72**, 3452 (1994). See also B.J. King (NEVIS Report 284) and C. Arroyo (NEVIS Report 293), Ph.D. Theses, Columbia University
5. W.J. Marciano and A. Sirlin, Phys. Rev. **D22**, 2695 (1980)
6. R.G. Stuart, Z. Phys. **C34**, 445 (1987)
7. Particle Data Group, Phys. Rev. **D54**, 85 (1996)
8. S.A. Rabinowitz et al., Phys. Rev. Lett. **70**, 134 (1993)
9. A. Romosan et al., NEVIS-1529, submitted to Phys. Rev. Lett (1996)
10. W.K. Sakumoto et al., Nucl. Inst. Meth. **A294**, 179 (1990)
11. B.J. King et al., Nucl. Inst. Meth. **A302**, 254 (1990)
12. F.S Merritt et al., Nucl. Inst. Meth. **A245**, 27 (1986); P.H. Sandler et al., Phys. Rev. **D42**, 759 (1990)
13. A.J. Buras and K.J.F. Gaemers, Nucl. Phys. **B132**, 249 (1978)
14. L.W. Whitlow. SLAC-Report-357, p.109 (1990)
15. P. Amaudruz et al., Nucl. Phys. **B371**, 3 (1992)
16. A. Baldit et al., Phys. Lett. **B332** 244 (1994)
17. M. Arneodo et al., Phys. Rev. **D50** 1 (1994)
18. D. Yu. Bardin and O.M. Fedorenko, Sov. J. Nucl. Phys **30**, 418 (1979); and private communication
19. J. Pumplin, Phys. Rev. Lett. **64** 2751 (1990).  $S_0 \leq 2 \text{ GeV}^2$  is allowed by data summarized in M. Virchaux and A. Milsztajn, Phys. Lett. **B274**, 221 (1992)
20. F. Abe et al., Phys. Rev. **D52** 4784 (1995); J. Lys for the CDF collaboration, proceedings of ICHEP 1996, FERMILAB-CONF-96-409-E; M. Rijssenbeek for the D0 collaboration, proceedings of ICHEP 1996, FERMILAB-CONF-96/365-E; S. Protopopescu for the D0 collaboration, proceedings of ICHEP 1996
21. G. Fogli, D. Haidt, Z. Phys. **C40**, 379 (1988)
22. E. Eichten, K. Lane and M. Peskin, Phys. Rev. Lett. **50**, 811 (1983)
23. A. Bodek for the CDF collaboration, proceedings of ICHEP 1996, University of Rochester Preprint, UR-1482 (ER/40685/894); CDF-3870